Published in final edited form as:
*FEBS J*. 2014 February ; 281(3): 957–969. doi:10.1111/febs.12661.

# Hyperoxia Increases the Elastic Modulus of Alveolar Epithelial Cells Through Rho Kinase

**Kristina R. Wilhelm**[*,1], **Esra Roan**[*,2], **Manik C. Ghosh**[1], **Kaushik Parthasarathi**[1], and **Christopher M. Waters**[1,3]

[1]Department of Physiology University of Tennessee Health Science Center Memphis, TN 38163

[3]Department of Medicine University of Tennessee Health Science Center Memphis, TN 38163

[2]Departments of Biomedical Engineering and Mechanical Engineering University of Memphis Memphis, TN 38152

## Abstract

Patients with acute lung injury are administered high concentrations of oxygen during mechanical ventilation, and while both hyperoxia and mechanical ventilation are necessary, each can independently cause additional injury. However, the precise mechanisms that lead to injury are not well understood. We hypothesized that alveolar epithelial cells may be more susceptible to injury caused by mechanical ventilation because hyperoxia causes cells to be stiffer due to increased f-actin formation via the GTPase RhoA and its effecter Rho kinase (ROCK). We examined cytoskeletal structures in cultured murine lung alveolar epithelial cells (MLE-12) under normoxic and hyperoxic (48h) conditions. We also measured cell elasticity (E) using atomic force microscopy (AFM) in the indenter mode. Hyperoxia caused increased f-actin stress fibers and bundle formation, an increase in g- and f-actin, an increase in nuclear area and a decrease in nuclear height, and cells became stiffer (higher E). Treatment with an inhibitor (Y-27632) of Rho kinase (ROCK) significantly decreased E and prevented the cytoskeletal changes, while it did not influence the nuclear height and area. Pre-exposure of cells to hyperoxia promoted detachment when cells were subsequently stretched cyclically, but the ROCK inhibitor prevented this effect. Hyperoxia caused thickening of vinculin focal adhesion plaques, and inhibition of ROCK reduced the formation of distinct focal adhesion plaques. Phosphorylation of focal adhesion kinase was significantly reduced by both hyperoxia and treatment with Y-27632. Hyperoxia caused increased cell stiffness and promoted cell detachment during stretch. These effects were ameliorated by inhibition of ROCK.

### Keywords

acute respiratory distress syndrome; atomic force microscopy; force maps; hyperoxia; alveolar epithelial cell; elastic modulus; RhoA; Rho kinase

## Introduction

Acute lung injury (ALI) and its more severe form acute respiratory distress syndrome (ARDS) are clinical conditions of acute respiratory failure. Patients with ALI/ARDS are administered high concentrations of oxygen (hyperoxia) during mechanical ventilation.

Address correspondence to: Christopher M. Waters, Ph.D. Department of Physiology The University of Tennessee Health Science Center 894 Union Ave, Room 426 Memphis, TN 38163-0001 Phone: (901) 448-5799 Fax: (901) 448-7126 cwaters2@uthsc.edu.
*both authors contributed equally

While both hyperoxia and mechanical ventilation are necessary, each can independently cause injury [1,2], and the combination accelerates the injury [3-6]. However, mechanical ventilation with supplemental oxygen remains the only therapy with a proven survival advantage, while numerous pharmacological therapies have failed to show benefits [7,8]. There has been extensive investigation of the signaling pathways that lead to lung injury after exposure to hyperoxia or mechanical ventilation, but the possibility that hyperoxia causes changes in mechanical properties of cells that promote lung injury during mechanical ventilation has not been extensively investigated [9].

The lung is cyclically distended during normal breathing, and it has been estimated that the alveolus undergoes a 4% linear distention of the basement membrane, while mechanical ventilation can cause distention between ~15% to 40% [10-12]. In ARDS the critical role of lung distention was illustrated by the landmark clinical trial by the ARDS network [7]. This study demonstrated a 22% reduction in mortality in ARDS patients when the tidal volume for mechanical ventilation was reduced from 12 ml/kg to 6 ml/kg predicted body weight. In vitro and in vivo studies suggest that the reduction in mortality may be associated with decreased biotrauma and biophysical injury by preventing or reducing over-distention of tissue, repetitive collapse and re-opening of airspaces, and injury caused by interfacial forces due to bubble propagation or foam [13-15].

Mechanical cues can be transmitted to the cells from the extracellular matrix (ECM), sensed directly by cellular deformation, or generated internally by the contractile cytoskeleton of individual cells [16,17]. Changes in the cell mechanical state through the contractile cytoskeleton highlight the fact that cells are dynamic, and therefore are able to respond to insults by activating signaling pathways or by adopting their mechanical properties.

We recently demonstrated that the resistance to mechanical deformation of murine lung alveolar epithelial cells (MLE-12) and primary rat alveolar epithelial cells (ATII) was significantly increased in response to hyperoxic conditions [9]. We further showed that hyperoxia-treated cells were more susceptible to stretch-induced injury (mimicking mechanical ventilation *in vivo*) due to the increased resistance to deformation of the cells. We measured the elastic modulus (E, or Young's modulus) using an atomic force microscope (AFM) in the indentation mode as an indication of the cells' resistance to deformation. While we showed that changes in E were linked to changes in the cytoskeleton, as suggested in other studies of cell mechanics [9,18,19], the mechanism for the changes in actin distribution were not investigated.

Actin assembly and contraction are regulated by the small Rho- family GTPases. Rho A regulates the assembly of actin and myosin stress fibers, the formation of focal contacts, and plays an important role in wound-closure and cell migration in general [20-22]. RhoA activates its downstream effector Rho kinase (ROCK) [23] that can be selectively inhibited by the pyridine derivative Y-27632 [24-26]. Even though it is known that Rho A is upregulated as a response to a variety of stressors such as exogenous factors [27], stretch [28,29], hypoxia [30] and hyperoxia [31,32], none of the previous studies have linked Rho A/ROCK to both an increase in E and f-actin formation.

In this study, we show that the hyperoxia-induced increase in elastic modulus is dependent upon both ROCK and an increase in actin. Cytoskeletal changes caused by hyperoxia included an increase in both globular actin (g-actin) and filamentous actin (f-actin). The hyperoxia-induced redistribution of cortical actin and the increase in E was blocked by inhibiting ROCK, and occurred independently of changes in nuclear size. We also show that ROCK inhibition prevented cell detachment caused by hyperoxia and mechanical stretch.

## Results

### Rock inhibition prevented hyperoxia-induced changes in f-actin

In our previous study we found that hyperoxia caused an increase in the elastic modulus (E) of cells that corresponded with an increase in f-actin filaments and cortical actin by fluorescence microscopy [9]. Treatment with cytochalasin D to disrupt f-actin prevented the hyperoxia-induced increase in E indicating that the increased stiffness of the cells was dependent upon the f-actin content. To test our hypothesis that changes in f-actin were dependent upon ROCK, we exposed MLE-12 cells to hyperoxia for 48hr in the presence or absence of the ROCK inhibitor Y-27632 and determined the changes in filamentous actin (f-actin) with rhodamine-phaloidin. Consistent with our previous results, we found that hyperoxia caused a thickening of cortical actin (Figure 1A-1B). Treatment of MLE-12 cells with Y-27632 reduced the thickness of the cortical actin in normoxia-treated cells (Figure 1C), and prevented the increase in cortical actin size in hyperoxia-treated cells (Figure 1D).

### Hyperoxia increased g-actin and f-actin

To further investigate the changes in actin after hyperoxia exposure, we measured the relative amounts of g-actin in the Triton-soluble fraction and f-actin associated with the cytoskeleton in the Triton-insoluble fraction. We hypothesized that the thickening in cortical actin that we observed would be accompanied by an increase in the f-actin content [33]. Representative western blots and densitometric analysis shown in Figure 2 indicate that the relative amount of f-actin was significantly increased in response to hyperoxia. However, when cells were treated with Y-27632 there was a significant decrease in f-actin in hyperoxia treated cells compared with untreated cells. Hyperoxia also caused a significant increase in g-actin content (Figure 2), but treatment with Y-27632 did not significantly affect g-actin content.

### ROCK inhibition did not affect hyperoxia-induced changes in nuclear area and height

Previous studies demonstrated that hyperoxia stimulated nuclear swelling in endothelial and epithelial cells [34-37]. We found that hyperoxia caused a significant increase in nuclear area (~67%) compared to control cells (Figure 3E), but nuclear height was significantly decreased (~23%, Figure 3F). These changes in nuclear area and height in response to hyperoxia were unaffected by treatment with Y-27632, indicating that ROCK inhibition did not influence the hyperoxia-induced changes in nuclear structure.

### ROCK inhibition ameliorated the hyperoxia-induced increase in elastic modulus

To determine whether hyperoxia-induced changes in E were due to activation of ROCK, we treated cells with Y-27632 during hyperoxia exposure and measured E. As in our previous study, hyperoxia caused a significant increase in E (Figure 4). Cells treated with Y-27632 under normoxia exhibited a significant decrease in E compared with control cells. Inhibition of ROCK prevented the hyperoxia-induced increase in E, and E in cells treated with Y27632 and hyperoxia were not significantly different from cells treated with Y27632 under normoxia conditions.

### ROCK inhibition reduced detachment of hyperoxia-treated cells due to cyclic stretch

In our previous study we found that cells with an increase in elastic modulus (less deformable) also had an increased susceptibility to injury caused by cyclic stretch [9]. Therefore, we hypothesized that the softening effect of Y-27632 would decrease the detachment of hyperoxia-treated cells during mechanical stretch. Approximately 1% of normoxia-treated cells detached during exposure to cyclic stretch (Figure 5), while ~24% of hyperoxia-treated cells detached during cyclic stretch. Hyperoxia alone caused increased cell

detachment relative to control cells, while there was no significant increase with Y-27632 treatment alone. Inhibition of ROCK in cells treated with hyperoxia significantly reduced the detachment of cells caused by cyclic stretch (6.4%) compared with cells treated with hyperoxia and stretch alone.

### Hyperoxia caused an increase in focal adhesion area

Since cell adhesion is regulated by focal adhesions, we investigated the expression and localization of vinculin in hyperoxia treated cells. The total amount of vinculin expressed in the cells did not change upon exposure to hyperoxia and/or inhibition of ROCK (Figure 6A). When we used immunofluorescence to determine the localization of vinculin, we observed prominent localization of vinculin in focal adhesions in both control and hyperoxia-treated cells, but focal adhesions in hyperoxia-treated cells appeared to be slightly larger, but fewer in number (Figure 6B-E). When we measured the area of the focal adhesions, we found that hyperoxia caused a small (13.6%) but significant increase in area (Fig. 6F). However, the density of focal adhesions was lower in hyperoxia treated cells (0.034 focal adhesions/$\mu m^2$) compared with control cells (0.052 focal adhesions/$\mu m^2$). Treatment with Y-27632 resulted in focal adhesions that were less well-defined in both control and hyperoxia-treated cells, which limited our ability to quantify them (Fig. 6D-E).

### FAK phosphorylation was decreased by both hyperoxia and inhibition of ROCK

Cell adhesion is mediated in part by focal adhesions, and focal adhesion kinase (FAK) is part of the complex of proteins that develops at focal adhesions. Previous studies have demonstrated a transient increase in FAK phosphorylation (pFAK, an indication of FAK activity) in response to oxidative stress [38-40]. We previously showed a decrease in pFAK (at tyrosine 397) in epithelial cells isolated from rats following exposure to hyperoxia and mechanical ventilation for 2 hr that correlated with decreased cell adhesion [41]. Since hyperoxia caused increased detachment of cells during cyclic stretch, we investigated whether hyperoxia affected pFAK. Figure 7, shows that hyperoxia caused a significant decrease in pFAK relative to total FAK. Interestingly, inhibition of ROCK also caused a decrease in pFAK in both normoxia and hyperoxia-treated cells.

## Discussion

We recently demonstrated that treatment of alveolar epithelial cells with hyperoxia caused an increase in the mechanical stiffness (E) of the cells that increased the susceptibility to stretch-induced injury [9], but the mechanism for this change in mechanical properties was not determined. We hypothesized that the observed increase in f-actin in the cells was due to RhoA/ROCK in response to hyperoxia-induced increase in reactive oxygen species. In the present study we demonstrated that inhibition of ROCK with Y-27632 reduced the hyperoxia-induced changes in f-actin (Figure 1 and Figure 2) and mechanical stiffness (Figure 4). We further showed that ROCK inhibition significantly decreased stretch-induced detachment of hyperoxia-treated cells (Figure 5).

We showed that hyperoxia increased f-actin qualitatively by fluorescence microscopy and quantitatively by western blot of Triton-insoluble cell lysates (Figures 1 and 2). Hyperoxia caused an increase in both g- and f-actin (Figure 2). Previous studies have shown an increase in f-actin content caused by oxidative stress including hydrogen peroxide [42,43] and hyperoxia [44,45]. In a previous study we found that the fraction of f-actin in Calu3 cells (an airway epithelial cell line) was initially decreased by exposure to hydrogen peroxide for 15 min, but a gradual rise in f-actin content occurred over 6 h [43]. DiPaolo et al. demonstrated that short term cyclic stretch stimulated actin remodeling in alveolar epithelial cells [46]. In the current study we focused on the effects of hyperoxia on actin and cell mechanical

properties and how these changes would affect subsequent exposure to cyclic stretch. However, it is possible that simultaneous exposure to both hyperoxia and cyclic stretch could cause different effects on cell structure and mechanical properties.

In our present and past studies [9] the amount of f-actin content correlated with the elastic modulus, and the increase in E and f-actin compared to control conditions are within the same order of magnitude. We also previously demonstrated that disruption of f-actin with cytochalasin D caused a significant decrease in the elastic modulus of cells. Others have also shown that cytoskeleton destabilization affects the elastic modulus [9,18,29,47,48], but we are the first to show the effect of Y-27632 on cell elasticity under hyperoxic conditions (Figure 4). Although the studies with cytochalasin D indicate that increased F-actin contributes to increased stiffness, Y-27632 can influence both F-actin content and actomyosin tone, so we cannot easily distinguish between these factors in the regulation of cell stiffness. It should also be noted that our AFM measurements of E in both normoxia- and hyperoxia-treated cells required approximately one hour under normoxic conditions, but we did not detect any changes in E during this time. This suggests that the time course of potential recovery of E following hyperoxia treatment was prolonged relative to this time frame. In future studies we will investigate these changes. Our results support the concept that although the elastic modulus is determined by the interactions among many different sub-cellular structures, cytoskeletal f-actin appears to be a major determinant of the mechanical response of lung epithelial cells to deformation.

Because the nucleus is the largest cell organelle, there has been particular interest in defining its role in determining the overall mechanical properties of a cell. While the majority of studies [49-51] suggest that the elastic modulus of the nucleus is about 3-10 times higher than that of the cytoplasm, some authors suggest that the cell nucleus has a lower elastic modulus than the cytoplasm [47]. These opposite results could potentially be explained by differences in cell types or by differences in measurement techniques. In the present study, we observed an increase in elastic modulus with hyperoxia, but we also measured an increase in nuclear area and a decrease in nuclear height. Furthermore, it should be pointed out that when MLE-12 cells are grown to confluence, the cells pack in closely and have a large proportion of area occupied by the nucleus. We did not measure the nuclear stiffness separately in this study, so we cannot rule out the possibility that changes in nuclear stiffness occurred. However, because we use an indentation depth of less than 300 nm and the cells are relatively tall, we are confident that our measurements of elastic modulus are more dependent upon the cytoskeleton and less upon the nucleus.

Our results showing an increase in nuclear area with hyperoxia treatment are consistent with previous reports [34-37]. Interestingly, while treatment with Y-27632 prevented changes in actin and elastic modulus, it had no effect on the hyperoxia-induced increase in the nuclear area or the reduction in height. Hyperoxia induced a ~67% increase in nuclear area (Figure 3E) and a reduction in nuclear height of ~ 23% (Figure 3G). If we assume the nucleus is disk-shaped, we estimate that the nuclear volume ($V= r^2h$) increased by 29%. Previous studies have demonstrated physical linkage between the nucleus and the cytoskeleton [49,52], and that actomyosin tension could affect nuclear height [53]. Lowering actomyosin tension, by inhibiting myosin II resulted in increased nuclear height [52]. However, in our study we did not observe a change in height due to Y-27632, indicating that the hyperoxia-induced decrease in height is unlikely to be related to an increase in cytoskeletal tension. Actin is not only one of the key structural elements of the cytoskeleton, but it is also one of the main components of the nuclear structure – the nucleoskeleton [54]. Nuclear actin, in contrast to cytoplasmic actin, does not form filaments and is predominately monomeric, but can form rods in response to stressors, e.g., heat shock treatment or ATP depletion [54]. Our results clearly demonstrate that ROCK inhibition influenced both the amount of cytoplasmic

f- and g-actin and E, but did not appear to influence the nuclear area and height (Figure 6E, F). The fact that Y-27632 influenced the amount of f-actin and the elastic modulus but not the nuclear area and height suggests that the Rho/ROCK pathway was not involved in nuclear size regulation in response to hyperoxia.

We recognize that there is a limitation in our measurements in that we assessed the nuclear area and height separately and not in relation to changes in cellular area and height. Increased volume (hypertrophy) upon hyperoxia exposure has been previously described in endothelial cells [55,56]. Although there was an apparent increase in cell area with hyperoxia treatment (Figures 1 and 5), we did not measure this directly. Instead, we estimated the cell size by counting the number of nuclei per unit area in a limited number of fields (n=4) from different treatments. Using this approach, we estimate a nearly 3-fold increase in cell area with hyperoxia treatment. Treatment with Y-27632 had no effect on cell size in control cells, but cells treated with hyperoxia in the presence of Y-27632 exhibited a 2-fold increase in cell area.

We previously proposed that the hyperoxia-induced increase in mechanical stiffness of cells would make them more susceptible to injury caused by mechanical stretch because stresses at cell-cell and cell-substrate contacts would be increased [9]. We confirmed this by measuring detachment of cells following cyclic stretch (Figure 5 and Roan et al. [9]). In the current study, when we treated cells with Y-27632 there was a significant decrease in the amount of cell detachment in hyperoxia-treated cells, suggesting that tension at contacts was reduced. Since focal adhesions are regulated in part by actomyosin-generated forces [57,58], we expected that hyperoxia would increase focal adhesion plaques in conjunction with an increase in f-actin (Figures 1 and 2). Thickening of focal adhesions following hyperoxia treatment has been described previously in endothelial cells [44]. In the current study, focal adhesion plaque area increased upon hyperoxia exposure by 13% (Figure 6B, C, F), possibly indicating an increased cytoskeletal tension [59]. However, the density of focal adhesions was reduced following hyperoxia (0.052 focal adhesions/$\mu m^2$ for control vs. 0.034 focal adhesions/$\mu m^2$ for hyperoxia). Inhibition of ROCK reduced the formation of distinct focal adhesions in both control and hyperoxia-treated cells. Since cell detachment was highest following hyperoxia treatment, we believe that the increased size of focal adhesions coupled with the reduced density causes a greater concentration of stress at these locations. We speculate that when deforming stress is applied, these sites of greater stress concentration are more likely to undergo failure and allow cell detachment. The reduced tension in cells treated with Y-27632 prevents the stress concentration and allows the cells to withstand deformation. Previous studies have demonstrated either increased or decreased phosphorylation of FAK in response to oxidative stress, depending upon the type of cell and the type of oxidative stress (reviewed in [39]). We found that hyperoxia caused a significant decrease in FAK phosphorylation at tyr397, and ROCK inhibition caused a further decrease (Figure 7). Since reduced phosphorylation at try397 did not correlate with increased cell detachment with stretch, FAK tyr397 phosphorylation does not appear to regulate strength of attachment. Earlier studies have also demonstrated that inhibition of ROCK reduced the formation of focal adhesions in control and hyperoxia treated cells (Figure 6D, E) [23,58], but to our knowledge it has not been shown that this protects cells against stretch-induced detachment.

Utilizing, a ventilator-induced lung injury model Birukova et al. recently showed that stretch-induced loss of endothelial barrier function could be attenuated by treatment with Y-27632 [60], and protective effects were also observed in other lung injury models [61,62]. We speculate that in addition to the other effects of ROCK inhibition in reducing lung injury, the prevention of cell stiffening is beneficial in reducing cell injury and detachment when lungs undergo cyclic distention. When ARDS patients are treated with hyperoxia, we

propose that cells become mechanically stiffer and that mechanical ventilation causes over-distention of tissue in some regions leading to greater injury. One limitation to this concept is that hyperoxia may also lead to changes in the composition and mechanical properties of the basement membrane, and this may also alter the cell-substrate interactions, potentially reducing the stress if the tissue also becomes stiffer. We did not investigate potential changes in the underlying matrix in response to hyperoxia in this study, but since inhibition of ROCK reduced cell detachment in hyperoxia-treated cells, potential changes in matrix are not likely to contribute to the response. Another potential factor in the response to hyperoxia is the stimulation of apoptosis [35,63]. De Paepe et al. examined the response of MLE-12 cells to hyperoxia and found that 48 hr of exposure resulted in ~17% TUNEL positive cells [63]. We did not specifically examine biochemical markers of apoptosis in this study, but there was not a substantial increase in nuclear fragmentation or apoptotic bodies after 48 hr of hyperoxia, and cell viability was >90%. In addition, the hyperoxia-induced increase in stiffness did not occur in Y-27632-treated cells. However, we cannot rule out the possibility that there was an increase in stiffness of some cells due to apoptosis.

In summary, we showed that hyperoxia increased stiffness in a cell line of lung alveolar epithelial cells, and that this effect was dependent on ROCK. By inhibiting this pathway, we reduced changes in f-actin and the elastic modulus of cells. Reducing the changes in cell stiffness led to decreased injury caused by stretch. These results could point toward improved strategies for reducing ventilator-induced lung injury.

## Materials and Methods

### Cell culture

The mouse alveolar epithelial cell line (MLE-12) [American Type Culture Collection (ATCC), Manassas, VA] was cultured in MLE-12 culture medium (DMEM with 10% heat-inactivated FBS, 1mM glutamine, 1% penicillin/streptomycin, 2% HEPES). The plating density was $0.7\times10^6$ cells/ml. Once confluent cells were exposed to either hyperoxia [~80–90% $O_2$, 5% $CO_2$, balance $N_2$; in a hyperoxia chamber (model: C374) from BioSpherix (Lacona, NY, USA), with an oxygen controller from the same company: Pro-ox: Model C21] or normoxia (with 5% $CO_2$) with or without the inhibitor of the Rho-associated protein kinase (Y-27632 – 40μM in 60 mm AFM-dishes or 20μM in 35 mm for 6 well plates, Tocris Bioscience, Missouri, USA) for 48h. Cells were then rinsed three times and transferred immediately to the AFM, or fixed for microscopy, or subjected to cell stretch experiments. Preliminary experiments with hyperoxia-treated cells demonstrated a dose-dependent decrease in E with Y-27632 treatment, and we used concentrations in the range of 20 to 40 μM because these were the lowest doses that had maximal effect on E. In all experiments cell viability was >90% [64].

### Fluorescence staining and confocal microscopy

Following treatment, monolayers were fixed in 10% formalin for 10 min and stained for f-actin using rhodamine-phalloidin (Cytoskeleton, Denver, CO, USA), according to the manufacturer's protocol. A 1:250 dilution was applied for one 1h. Nuclear staining was obtained using Hoechst 333423 (1:1.000, Invitrogen, Grant Island, NY, USA) for 5min. In order to visualize focal adhesions we stained for vinculin on cells grown on glass cover slips. Following treatment, cells were fixed with 4% paraformaldehyde for 5 min, and stained over night with a vinculin antibody conjugated to FITC (Sigma – Aldrich, St. Louis, MO, USA) in a 1:100 dilution at 4°C. Images were acquired on a Zeiss 710 (Zeiss, Jena, Germany) laser confocal inverted microscope with six laser lines on a 40X (actin, nuclear area) or 63X (vinculin, nuclear height) objective, using the Zen 2010 software. Analysis of focal adhesion area was performed with ImageJ 1.46r image processing software (W.S.

Rasband; NIH, Bethesda, MD; http://rsbweb.nih.gov/ij/). All focal adhesion images for control and hyperoxia cells were recorded with the same settings. Based upon the appearance of the focal adhesion plaques, areas between 10-100 pixel$^2$ were used in the analysis.

### Nuclear area and height measurements

All nuclear measurements were performed on fixed cells. Nuclear areas were outlined and measured using ImageJ 1.46r image processing software. For each condition, a minimum of 130 individual nuclei were outlined and measured from wells from three different experiments with at least three different fields from each well. If nuclei were directly adjacent, they were separated for analysis by manually outlining them. The nuclear area was then calculated using ImageJ. To create a height image of the DAPI stained nucleus we used z-stack images with a step width of 1 m. We performed 4 independent experiments; in every experiment at least 5 images were analyzed, between 4-5 nuclei in each image. This resulted in around 100 analyzed nuclei per condition.

### Measurement of cytoskeletal association of actin

Actin was extracted as described previously [42,43] and separated as follows: 1) monomeric actin (g-actin) and a small amount of filamentous actin (f-actin) not cross-linked to the cytoskeleton were soluble in Triton X-100; and 2) f-actin fibers attached to the cytoskeleton were insoluble in Triton X-100. Cells on 6-well culture plates were placed on ice and washed once with cold PBS containing magnesium and calcium. Cells were then lysed with 500 μl ice-cold extraction buffer (1% Triton X-100, 20mM Tris, 5 mM EGTA, 20mM sodium fluoride, 25 mM sodium pyrophosphate and protease inhibitor, ph 7.4) for 5 min. Afterwards the wells were washed twice with PBS, and filamentous f-actin was extracted with 500 μl depolymerization buffer (extraction buffer with 5% SDS, 5% deoxycholic). F-actin samples were incubated in depolymerization buffer at 4°C for 30 min with gentle shaking, and then centrifuged for 15 min. The supernatant was collected, and all samples were boiled in Lammeli buffer for 5 min.

### Western blot analysis

The relative amounts of g- and f-actin and phosphorylated, total focal adhesion kinase (pFAK and t-FAK) and vinculin were determined using Western analysis. The gel electrophoresis and transfer protocols were performed following the standard protocols of the NuPAGE electrophoresis system (Novex, San Diego, CA, USA) using a 4 – 12% Bis-Tris gel with MOPS running buffer under reducing conditions. Actin was detected using a standard immunodetection protocol with a 1:1000 dilution of rabbit anti-actin antibody (Cytoskeleton, Denver, CO, USA) and HRP-conjugated goat anti-rabbit secondary antibody (1:3.000) (Cell Signaling, Danvers, MA, USA). Because of the two step extraction process, samples were loaded with specific volumes (based upon dilutions) rather than with equal protein. We used GAPDH as a loading control for the Triton-soluble fraction (g-actin), and we ran the samples for g- and f-actin on the same gel. Immunoblots for pFAK and total FAK were performed using an antibody for pFAK (against phosphorylated Y397, abCam, MA) using a 1:500 dilution incubated overnight followed by stripping and probing for total FAK using an antibody (Cell Signaling, MA) at a dilution of 1:5000 incubated for 1 hr. Vinculin immunoblots were performed using an antibody for vinculin (Sigma-Aldrich, St. Louis, MO, USA) in 1:5000 dilution incubated over night and HRP-conjugated goat anti-rabbit secondary antibody (1:10.000). GAPDH was used as a loading control. Bands were visualized by enhanced chemiluminescence with ECL reagent (Millipore, Billerica, MA, USA). All experiments were repeated 3 to 4 times. Densitometry of bands was performed using ImageJ 1.46r software to determine relative quantities of g- and f-actin, GAPDH, pFAK, total FAK, and vinculin. Since g- and f-actin were extracted from the same well,

GAPDH was used as a loading control for only g-actin (both f- and g-actin were run on the same gel). Although long term exposure to hyperoxia can change the expression of GAPDH [65,66], we have not observed a significant change in expression in MLE-12 cells during 48 hr of exposure.

To account for variability between immunoblots the values within a given experiment (from the same blot) were normalized to the normoxia condition. The densitometry for all other bands was evaluated for each condition and expressed relative to GAPDH or to total FAK.

### Atomic force microscopy

To measure the elastic modulus of cells, we utilized an AFM (Asylum Research, Santa Barbara, CA, MFP3D3) as a nano-indenter with a flexible cantilever beam, as others and we have described previously [9,67,68]. Once the cells were treated according to our experimental groups, we removed the cells from the incubator and placed them in the AFM chamber. At a minimum, we conducted 142 measurements at 20 locations in a single petri dish, adding up to over 2800 independent force-indentation curves. We analyzed each force-indentation curve with our MATLAB code to determine the E at a given location, and then we obtained a median for each field [9,67,68]. We then averaged the median values from each field to obtain the overall E for the dish. We repeated these measurements for three cell seeding events. Because of variations with the tips, we normalized E for each condition in a given experiment to the E value for control (normoxia) cells.

### Cell detachment

Confluent monolayers of MLE-12 cells were exposed to either normoxia or hyperoxia with or without Y-27632 for 48h as described above and then exposed to cyclic stretch using the Flexercell FX-4000T tension unit (Flexcell International, Hillsborough, NC). Cells were exposed to 20% linear strain for 60 min at a frequency of 15 cycles/min. We choose 20% strain to simulate the high distention that can occur during mechanical ventilation in injured lungs [10]. Cells were then fixed in 10% formalin for 5 min, and phase-contrast images were collected at 10X magnification using an EVOS microscope (Advanced Microscopy Group, Bothell, WA) with three to five fields for each well. The images were then analyzed using Photoshop and Matlab software. Areas of cell detachment were detected by the operator and outlined automatically by Photoshop, and Matlab was used to determine the percentage of denuded area with respect to the overall field. Non-stretched cells were used as controls, and measurements of each condition were made from three different experiments.

### Statistical analysis

We utilized SigmaPlot (Systat Software) for the statistical analysis. Values for measurements of densitometry, nuclear area, elastic modulus, and area of denuded cells are given as means +/− the standard error or the mean. Measurements were made from at three to four independent experiments. A t-test was used when only two groups were compared, and one-way or two-way ANOVA with the Holm-Sidak method was used for comparisons of multiple treatments to determine significant differences between individual conditions. If equal variance was not satisfied, then ANOVA on ranks was performed and comparisons were made using Dunn's method. In the analysis of cell detachment data, three-way ANOVA was used to determine significant differences and interactions among the different treatments. Significant differences were determined based on a threshold of $P < 0.05$.

## Acknowledgments

This work was supported by NIH grant HL094366. We thank Charlean L. Luellen, Bin Teng, Amanda Preston and Gabriel Rapalo at the University of Tennessee Health Science Center for help, advice, and technical assistance. We

thank Hummad Tasneem at the University of Memphis for help with data analysis. We thank Dr. Lindner and Dr. Pinkhasshik at the University of Memphis for the unlimited access to the AFM.

## Abbreviations

| | |
|---|---|
| **AFM** | atomic force microscopy |
| **ALI** | acute lung injury |
| **ARDS** | acute respiratory distress syndrome |
| **ATII** | type II alveolar epithelial cells |
| **E** | elastic modulus |
| **ECM** | extracellular matrix |
| **FAK** | focal adhesion kinase |
| **ROCK** | Rho kinase. |

## References

1. Zaher TE, Miller EJ, Morrow DM, Javdan M, Mantell LL. Hyperoxia-induced signal transduction pathways in pulmonary epithelial cells. Free Radic Biol Med. 2007; 42:897–908. [PubMed: 17349918]
2. Pagano A, Barazzone-Argiroffo C. Alveolar cell death in hyperoxia-induced lung injury. Ann N Y Acad Sci. 2003; 1010:405–416. [PubMed: 15033761]
3. Makena PS, Luellen CL, Balazs L, Ghosh MC, Parthasarathi K, et al. Preexposure to hyperoxia causes increased lung injury and epithelial apoptosis in mice ventilated with high tidal volumes. Am J Physiol Lung Cell Mol Physiol. 2010; 299:L711–719. [PubMed: 20833778]
4. Bailey TC, Martin EL, Zhao L, Veldhuizen RA. High oxygen concentrations predispose mouse lungs to the deleterious effects of high stretch ventilation. J Appl Physiol. 2003; 94:975–982. [PubMed: 12571129]
5. Davis JM, Penney DP, Notter RH, Metlay L, Dickerson B, et al. Lung injury in the neonatal piglet caused by hyperoxia and mechanical ventilation. J Appl Physiol. 1989; 67:1007–1012. [PubMed: 2793694]
6. Li LF, Liao SK, Ko YS, Lee CH, Quinn DA. Hyperoxia increases ventilator-induced lung injury via mitogen-activated protein kinases: a prospective, controlled animal experiment. Crit Care. 2007; 11:R25. [PubMed: 17316425]
7. Brower RG, Matthay MA, Morris A, Schoenfeld D, Thompson BT, et al. Ventilation with lower tidal volumes as compared with traditional tidal volumes for acute lung injury and the acute respiratory distress syndrome. New England Journal of Medicine. 2000; 342:1301–1308. [PubMed: 10793162]
8. Levitt JE, Matthay MA. The utility of clinical predictors of acute lung injury: towards prevention and earlier recognition. Expert Rev Respir Med. 2010; 4:785–797. [PubMed: 21128753]
9. Roan E, Wilhelm K, Bada A, Makena PS, Gorantla VK, et al. Hyperoxia alters the mechanical properties of alveolar epithelial cells. Am J Physiol Lung Cell Mol Physiol. 2012; 302:L1235–1241. [PubMed: 22467640]
10. Roan E, Waters CM. What do we know about mechanical strain in lung alveoli? Am J Physiol Lung Cell Mol Physiol. 2011; 301:L625–635. [PubMed: 21873445]
11. Fredberg JJ, Kamm RD. Stress transmission in the lung: pathways from organ to molecule. Annu Rev Physiol. 2006; 68:507–541. [PubMed: 16460282]
12. Tschumperlin DJ, Margulies SS. Equibiaxial deformation-induced injury of alveolar epithelial cells in vitro. Am J Physiol. 1998; 275:L1173–1183. [PubMed: 9843855]
13. Oeckler RA, Hubmayr RD. Cell wounding and repair in ventilator injured lungs. Respir Physiol Neurobiol. 2008; 163:44–53. [PubMed: 18638574]

14. Ghadiali SN, Gaver DP. Biomechanics of liquid-epithelium interactions in pulmonary airways. Respir Physiol Neurobiol. 2008; 163:232–243. [PubMed: 18511356]
15. Hussein O, Walters B, Stroetz R, Valencia P, McCall D, et al. Biophysical determinants of alveolar epithelial plasma membrane wounding associated with mechanical ventilation. Am J Physiol Lung Cell Mol Physiol. 2013; 305:L478–L484. [PubMed: 23997173]
16. Chen CS. Mechanotransduction - a field pulling together? J Cell Sci. 2008; 121:3285–3292. [PubMed: 18843115]
17. Matthews BD, Overby DR, Mannix R, Ingber DE. Cellular adaptation to mechanical stress: role of integrins, Rho, cytoskeletal tension and mechanosensitive ion channels. J Cell Sci. 2006; 119:508–518. [PubMed: 16443749]
18. Ketene AN, Roberts PC, Shea AA, Schmelz EM, Agah M. Actin filaments play a primary role for structural integrity and viscoelastic response in cells. Integr Biol (Camb). 2012; 4:540–549. [PubMed: 22446682]
19. Walter N, Busch T, Seufferlein T, Spatz JP. Elastic moduli of living epithelial pancreatic cancer cells and their skeletonized keratin intermediate filament network. Biointerphases. 2011; 6:79–85. [PubMed: 21721843]
20. Desai LP, Aryal AM, Ceacareanu B, Hassid A, Waters CM. RhoA and Rac1 are both required for efficient wound closure of airway epithelial cells. Am J Physiol Lung Cell Mol Physiol. 2004; 287:L1134–1144. [PubMed: 15298851]
21. Evers EE, Zondag GC, Malliri A, Price LS, ten Klooster JP, et al. Rho family proteins in cell adhesion and cell migration. Eur J Cancer. 2000; 36:1269–1274. [PubMed: 10882865]
22. Hoffman BD, Crocker JC. Cell mechanics: dissecting the physical responses of cells to force. Annu Rev Biomed Eng. 2009; 11:259–288. [PubMed: 19400709]
23. Riento K, Ridley AJ. Rocks: multifunctional kinases in cell behaviour. Nat Rev Mol Cell Biol. 2003; 4:446–456. [PubMed: 12778124]
24. Davies SP, Reddy H, Caivano M, Cohen P. Specificity and mechanism of action of some commonly used protein kinase inhibitors. Biochem J. 2000; 351:95–105. [PubMed: 10998351]
25. Narumiya S, Ishizaki T, Uehata M. Use and properties of ROCK-specific inhibitor Y-27632. Regulators and Effectors of Small Gtpases. 2000; 325:273–284. Pt D.
26. Uehata M, Ishizaki T, Satoh H, Ono T, Kawahara T, et al. Calcium sensitization of smooth muscle mediated by a Rho-associated protein kinase in hypertension. Nature. 1997; 389:990–994. [PubMed: 9353125]
27. Ramseyer VD, Hong NJ, Garvin JL. Tumor necrosis factor alpha decreases nitric oxide synthase type 3 expression primarily via Rho/Rho kinase in the thick ascending limb. Hypertension. 2012; 59:1145–1150. [PubMed: 22566503]
28. Foster CD, Varghese LS, Gonzales LW, Margulies SS, Guttentag SH. The Rho pathway mediates transition to an alveolar type I cell phenotype during static stretch of alveolar type II cells. Pediatr Res. 2010; 67:585–590. [PubMed: 20220547]
29. DiPaolo BC, Margulies SS. Rho kinase signaling pathways during stretch in primary alveolar epithelia. Am J Physiol Lung Cell Mol Physiol. 2012; 302:L992–1002. [PubMed: 22287611]
30. Rousseau M, Gaugler MH, Rodallec A, Bonnaud S, Paris F, et al. RhoA GTPase regulates radiation-induced alterations in endothelial cell adhesion and migration. Biochem Biophys Res Commun. 2011; 414:750–755. [PubMed: 22001926]
31. Kondrikov D, Caldwell RB, Dong Z, Su Y. Reactive oxygen species-dependent RhoA activation mediates collagen synthesis in hyperoxic lung fibrosis. Free Radic Biol Med. 2011; 50:1689–1698. [PubMed: 21439370]
32. Desai LP, Sinclair SE, Chapman KE, Hassid A, Waters CM. High tidal volume mechanical ventilation with hyperoxia alters alveolar type II cell adhesion. American Journal of Physiology-Lung Cellular and Molecular Physiology. 2007; 293:L769–L778. [PubMed: 17601798]
33. Totsukawa G, Yamakita Y, Yamashiro S, Hartshorne DJ, Sasaki Y, et al. Distinct roles of ROCK (Rho-kinase) and MLCK in spatial regulation of MLC phosphorylation for assembly of stress fibers and focal adhesions in 3T3 fibroblasts. J Cell Biol. 2000; 150:797–806. [PubMed: 10953004]

34. Romashko J 3rd, Horowitz S, Franek WR, Palaia T, Miller EJ, et al. MAPK pathways mediate hyperoxia-induced oncotic cell death in lung epithelial cells. Free Radic Biol Med. 2003; 35:978–993. [PubMed: 14556862]
35. Mantell LL, Lee PJ. Signal transduction pathways in hyperoxia-induced lung cell death. Mol Genet Metab. 2000; 71:359–370. [PubMed: 11001828]
36. Phillips PG, Higgins PJ, Malik AB, Tsan MF. Effect of hyperoxia on the cytoarchitecture of cultured endothelial cells. Am J Pathol. 1988; 132:59–72. [PubMed: 3394802]
37. Lee SL, Douglas WH, Deneke SM, Fanburg BL. Ultrastructural changes in bovine pulmonary artery endothelial cells exposed to 80% O2 in vitro. In Vitro. 1983; 19:714–722. [PubMed: 6413390]
38. Vepa S, Scribner WM, Parinandi NL, English D, Garcia JG, et al. Hydrogen peroxide stimulates tyrosine phosphorylation of focal adhesion kinase in vascular endothelial cells. Am J Physiol. 1999; 277:L150–158. [PubMed: 10409242]
39. Ben Mahdi MH, Andrieu V, Pasquier C. Focal adhesion kinase regulation by oxidative stress in different cell types. IUBMB Life. 2000; 50:291–299. [PubMed: 11327323]
40. Aghajanian A, Wittchen ES, Campbell SL, Burridge K. Direct activation of RhoA by reactive oxygen species requires a redox-sensitive motif. PLoS One. 2009; 4:e8045. [PubMed: 19956681]
41. Desai LP, Sinclair SE, Chapman KE, Hassid A, Waters CM. High tidal volume mechanical ventilation with hyperoxia alters alveolar type II cell adhesion. Am J Physiol Lung Cell Mol Physiol. 2007; 293:L769–778. [PubMed: 17601798]
42. Zhao Y, Davis HW. Hydrogen peroxide-induced cytoskeletal rearrangement in cultured pulmonary endothelial cells. J Cell Physiol. 1998; 174:370–379. [PubMed: 9462699]
43. Boardman KC, Aryal AM, Miller WM, Waters CM. Actin re-distribution in response to hydrogen peroxide in airway epithelial cells. J Cell Physiol. 2004; 199:57–66. [PubMed: 14978735]
44. Phillips PG, Birnby L, Di Bernardo LA, Ryan TJ, Tsan MF. Hyperoxia increases plasminogen activator activity of cultured endothelial cells. Am J Physiol. 1992; 262:L21–31. [PubMed: 1733278]
45. Kondrikov D, Elms S, Fulton D, Su Y. eNOS-beta-actin interaction contributes to increased peroxynitrite formation during hyperoxia in pulmonary artery endothelial cells and mouse lungs. J Biol Chem. 2010; 285:35479–35487. [PubMed: 20826796]
46. DiPaolo BC, Lenormand G, Fredberg JJ, Margulies SS. Stretch magnitude and frequency-dependent actin cytoskeleton remodeling in alveolar epithelia. American Journal of Physiology - Cell Physiology. 2010; 299:C345–C353. [PubMed: 20519449]
47. Martens JC, Radmacher M. Softening of the actin cytoskeleton by inhibition of myosin II. Pflugers Arch. 2008; 456:95–100. [PubMed: 18231808]
48. Pelling AE, Dawson DW, Carreon DM, Christiansen JJ, Shen RR, et al. Distinct contributions of microtubule subtypes to cell membrane shape and stability. Nanomedicine. 2007; 3:43–52. [PubMed: 17379168]
49. Maniotis AJ, Chen CS, Ingber DE. Demonstration of mechanical connections between integrins cytoskeletal filaments, and nucleoplasm that stabilize nuclear structure. Proceedings of the National Academy of Sciences of the United States of America. 1997; 94:849–854. [PubMed: 9023345]
50. Guilak F, Tedrow JR, Burgkart R. Viscoelastic properties of the cell nucleus. Biochem Biophys Res Commun. 2000; 269:781–786. [PubMed: 10720492]
51. Caille N, Thoumine O, Tardy Y, Meister JJ. Contribution of the nucleus to the mechanical properties of endothelial cells. J Biomech. 2002; 35:177–187. [PubMed: 11784536]
52. Chancellor TJ, Lee J, Thodeti CK, Lele T. Actomyosin tension exerted on the nucleus through nesprin-1 connections influences endothelial cell adhesion, migration, and cyclic strain-induced reorientation. Biophys J. 2010; 99:115–123. [PubMed: 20655839]
53. Sims JR, Karp S, Ingber DE. Altering the cellular mechanical force balance results in integrated changes in cell, cytoskeletal and nuclear shape. J Cell Sci. 1992; 103(Pt 4):1215–1222. [PubMed: 1487498]
54. de Lanerolle P, Serebryannyy L. Nuclear actin and myosins: life without filaments. Nat Cell Biol. 2011; 13:1282–1288. [PubMed: 22048410]

55. Lei Y, Stamer WD, Wu J, Sun X. Oxidative stress impact on barrier function of porcine angular aqueous plexus cell monolayers. Invest Ophthalmol Vis Sci. 2013; 54:4827–4835. [PubMed: 23761078]
56. Das SK, Fanburg BL. TGF-beta 1 produces a "prooxidant" effect on bovine pulmonary artery endothelial cells in culture. Am J Physiol. 1991; 261:L249–254. [PubMed: 1928358]
57. Wolfenson H, Bershadsky A, Henis YI, Geiger B. Actomyosin-generated tension controls the molecular kinetics of focal adhesions. J Cell Sci. 2011; 124:1425–1432. [PubMed: 21486952]
58. Lavelin I, Wolfenson H, Patla I, Henis YI, Medalia O, et al. Differential effect of actomyosin relaxation on the dynamic properties of focal adhesion proteins. PLoS One. 2013; 8:e73549. [PubMed: 24039980]
59. Chen CS, Alonso JL, Ostuni E, Whitesides GM, Ingber DE. Cell shape provides global control of focal adhesion assembly. Biochem Biophys Res Commun. 2003; 307:355–361. [PubMed: 12859964]
60. Birukova AA, Tian Y, Meliton A, Leff A, Wu T, et al. Stimulation of Rho signaling by pathologic mechanical stretch is a "second hit" to Rho-independent lung injury induced by IL-6. Am J Physiol Lung Cell Mol Physiol. 2012; 302:L965–975. [PubMed: 22345573]
61. Cinel I, Ark M, Dellinger P, Karabacak T, Tamer L, et al. Involvement of Rho kinase (ROCK) in sepsis-induced acute lung injury. J Thorac Dis. 2012; 4:30–39. [PubMed: 22295165]
62. Tasaka S, Koh H, Yamada W, Shimizu M, Ogawa Y, et al. Attenuation of endotoxin-induced acute lung injury by the Rho-associated kinase inhibitor, Y-27632. Am J Respir Cell Mol Biol. 2005; 32:504–510. [PubMed: 15778497]
63. De Paepe ME, Mao Q, Chao Y, Powell JL, Rubin LP, et al. Hyperoxia-induced apoptosis and Fas/FasL expression in lung epithelial cells. Am J Physiol Lung Cell Mol Physiol. 2005; 289:L647–659. [PubMed: 16148053]
64. Schwingshackl A, Teng B, Ghosh M, West AN, Makena P, et al. Regulation and function of the two-pore-domain (K2P) potassium channel Trek-1 in alveolar epithelial cells. Am J Physiol Lung Cell Mol Physiol. 2012; 302:L93–L102. [PubMed: 21949155]
65. Shimada I, Matsui K, Iida R, Tsubota E, Matsuki T. Time course of housekeeping gene expression changes in diffuse alveolar damage induced by hyperoxia exposure in mice. Leg Med (Tokyo). 2009; 11(Suppl 1):S151–154. [PubMed: 19272828]
66. Kim I, Yang D, Tang X, Carroll JL. Reference gene validation for qPCR in rat carotid body during postnatal development. BMC Res Notes. 2011; 4:440. [PubMed: 22023793]
67. Lin DC, Dimitriadis EK, Horkay F. Robust strategies for automated AFM force curve analysis-II: adhesion-influenced indentation of soft, elastic materials. J Biomech Eng. 2007; 129:904–912. [PubMed: 18067395]
68. Rico F, Roca-Cusachs P, Gavara N, Farre R, Rotger M, et al. Probing mechanical properties of living cells by atomic force microscopy with blunted pyramidal cantilever tips. Phys Rev E Stat Nonlin Soft Matter Phys. 2005; 72:021914. [PubMed: 16196611]

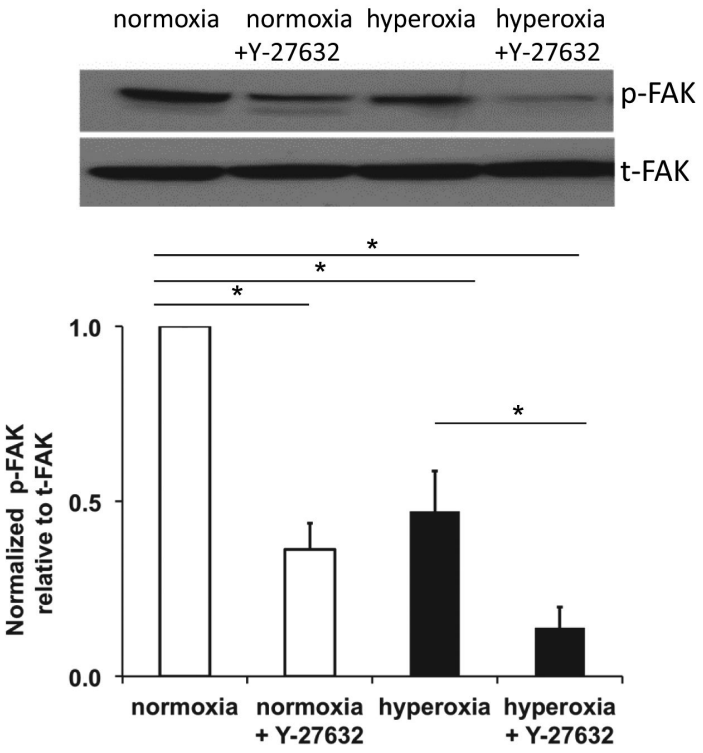


**Figure 1. ROCK inhibition prevented hyperoxia-induce changes in f-actin distribution**

Fluorescence images of F-actin in MLE-12 cells stained with rhodamine phaloidin. Compared to normoxia (A), hyperoxia for 48h (B) caused a thickening of the cortical F-actin and an increase in cell area. Treatment with the Rho Kinase inhibitor (Y-27632, 40 μM, C and D) prevented the changes in f-actin in the hyperoxia-treated cells (D). Scale bars are 50μm (representative images from 3 different experiments).

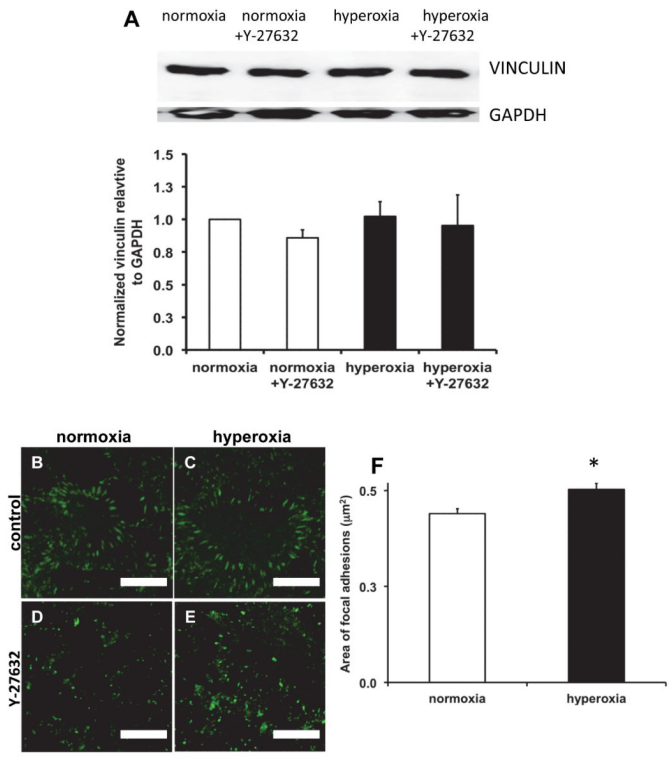


**Figure 2. Hyperoxia increased g-actin and f-actin content**

Representative western blots of g-actin and f-actin from the same well for each condition, and GAPDH as a loading control for g-actin (upper panel). Equivalent volumes from the Triton-soluble and Triton-insoluble fractions were loaded onto the same gel for comparison. The lower panel shows the densitometry for g-actin normalized to GAPDH and the densitometry for f-actin. Both g- and f-actin were further normalized to the normoxia condition. * indicates a significant difference, $p<0.05$; N.S. indicates not significant; n=4, error bars indicate standard error.

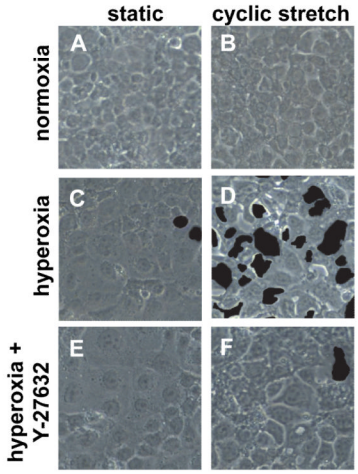


G

% cell denuded area:

| | static | stretch |
|---|---|---|
| normoxia | 0.4±0.5 | 1.1±0.5 |
| hyperoxia | 5.1±2.8 | 24.7±5.7* |
| normoxia +Y-27732 | 0.5±0.3 | 0.2±0.1 |
| hyperoxia +Y-27732 | 2.2±1.6 | 6.4±2.5** |

**Figure 3. Hyperoxia increased nuclear size, and ROCK inhibition did not prevent the increase**

Panel A: Fluorescence images of MLE-12 cells stained with Hoechst33342. Compared to normoxia (A), hyperoxia (B) caused nuclear swelling. Y-27632 did not influence nuclear size (C, D). Scale bars are 50μm. Panel E: Quantification of nuclear size in normoxia and hyperoxia treatment with and without Y-27632. Nuclei (>120) from 3-5 fields in 3 different experiments were measured. Panel F: Quantification of nuclear height in normoxia and hyperoxia treatment with and without Y-27632. Nuclei (~100) from 5 fields in 3-4 different experiments were measured. * indicates significant differences from normoxia treatment; $p<0.05$; error bars indicate standard error.

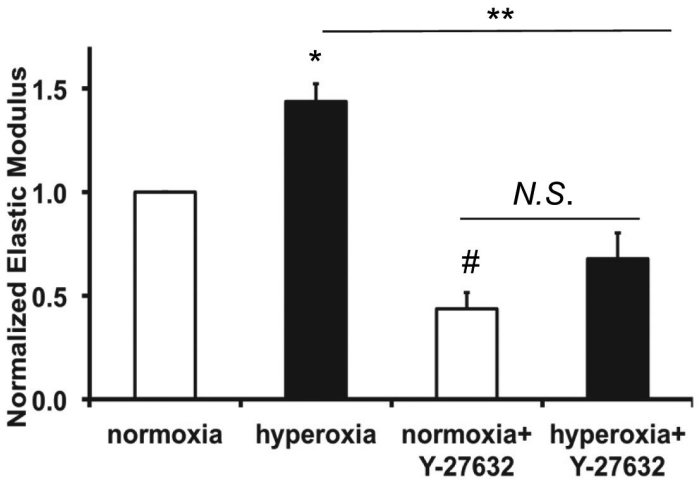


**Figure 4. ROCK inhibition reduced the hyperoxia-induced increase in elastic modulus**

Elastic moduli (E) were measured by AFM and normalized to the normoxia treated cells. Hyperoxia for 48 hr (HO) caused a significant increase in E compared to normoxia (NO); the increase was reduced in the presence of Y-27632. Y-27632 also caused a decreased E in normoxia treated cells relative to control. Each data point represents the mean value from 15 to 20 locations in a given dish in which the median value was determined from 144 measurements near that location, (n=3 different experiments). * indicates significant differences from normoxia treatment, # indicates significant differences between hyperoxia and hyperoxia +Y-27632 treatment; $p<0.05$, error bars indicate standard error; N.S. indicates no significant difference.

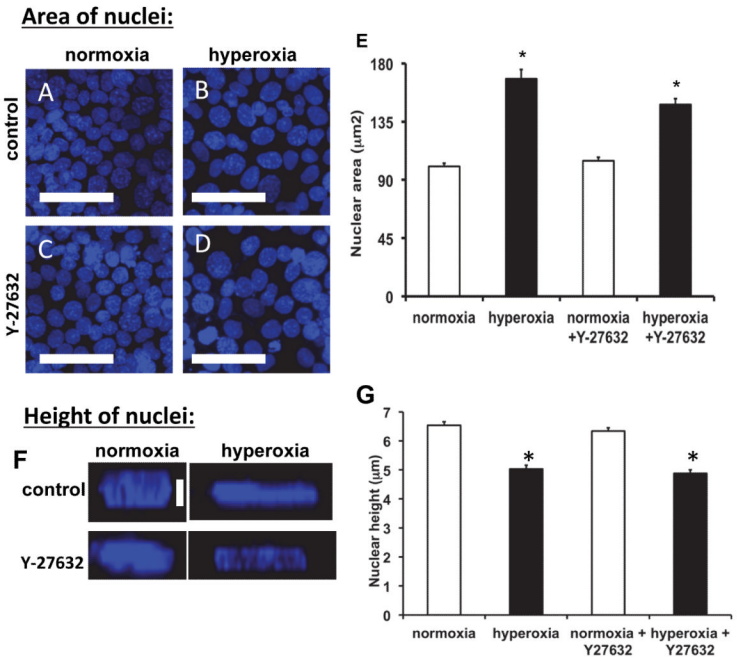


**Figure 5. Cyclic stretch caused detachment of hyperoxia-treated cells, and ROCK inhibition ameliorated this effect**

Cells were treated for 48 h with normoxia (A and B) or hyperoxia (C, D, E, and F) and then kept static (A, C, and E) or exposed to 20% cyclic stretch, 15 cycles/min (B, D, and F) for 60 min. Cells in E and F were treated with Y-27632 during the hyperoxia treatment. For Panels A-F areas of cell detachment were identified by the user, filled in automatically by Photoshop (indicated by dark areas), and quantified using Matlab as described in Methods. Panel G: Quantification of cell detachment: percentage of area of detached cells was determined for at least 5 fields from at least 3 different wells (n=3); three-way ANOVA was performed with the Holm-Sidak method used for comparisons; * indicates a significant difference from stretched, normoxia treated cells; ** indicates a significant difference from stretched, hyperoxia treated cells; $p<0.05$; standard errors are indicated.

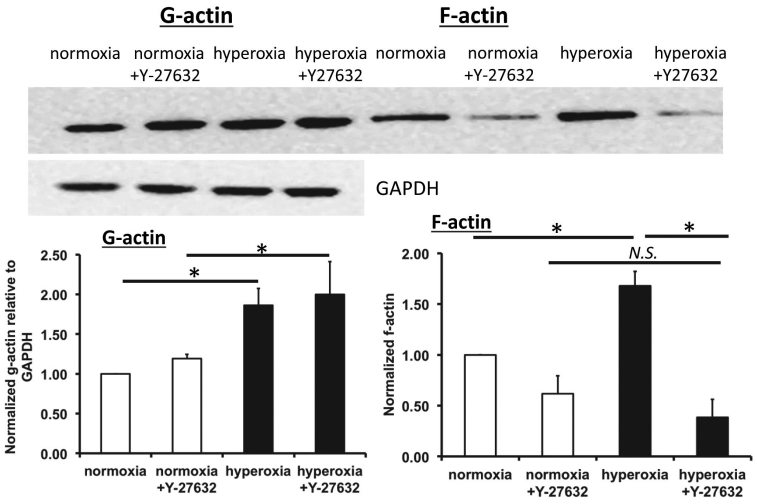


**Figure 6. Hyperoxia caused an increase in focal adhesion area but did not increase total vinculin**

Panel A: Representative western blots of vinculin and GAPDH and densitometry summarized from 3 experiments. Panels B-E: Immunofluorescence images of focal adhesions in MLE-12 cells stained for vinculin. Compared to normoxia (B), hyperoxia for 48h (C) caused a thickening of the focal adhesions. Treatment with the Rho Kinase inhibitor (Y-27632, D and E) reduced the localization of vinculin in both normoxia (D) and hyperoxia-treated (E) cells. Scale bars are 10μm (representative images from 3 different experiments). Panel F: Quantification of focal adhesion area in normoxia and hyperoxia-treated cells. Focal adhesions (>1500) from 5-7 fields for each condition in 3 different experiments were measured.

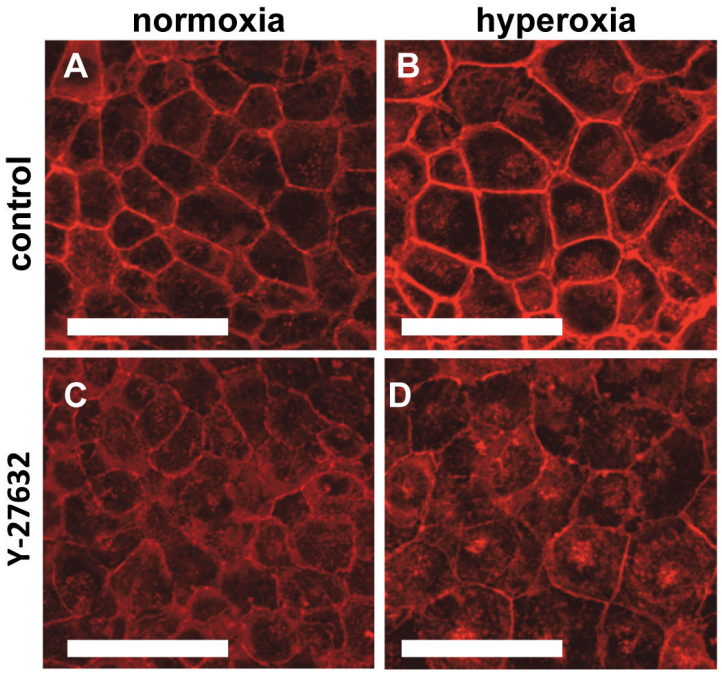


**Figure 7. Hyperoxia and ROCK inhibition decreased pFAK**

Representative western blots of pFAK and total FAK and densitometry summarized from 3 experiments. * indicates a significant difference, $p<0.05$; error bars indicate standard error.